

Metal nanoparticles restrict the growth of protozoan parasites

Oluoyomi Stephen Adeyemi, Nthatisi Innocentia Molefe, Oluwakemi Josephine Awakan, Charles Obiora Nwonuma, Omokolade Oluwaseyi Alejlowo, Tomilola Olaolu, Rotdelmwa Filibus Maimako, Keisuke Suganuma, Yongmei Han & Kentaro Kato

To cite this article: Oluoyomi Stephen Adeyemi, Nthatisi Innocentia Molefe, Oluwakemi Josephine Awakan, Charles Obiora Nwonuma, Omokolade Oluwaseyi Alejlowo, Tomilola Olaolu, Rotdelmwa Filibus Maimako, Keisuke Suganuma, Yongmei Han & Kentaro Kato (2018) Metal nanoparticles restrict the growth of protozoan parasites, *Artificial Cells, Nanomedicine, and Biotechnology*, 46:sup3, S86-S94, DOI: [10.1080/21691401.2018.1489267](https://doi.org/10.1080/21691401.2018.1489267)

To link to this article: <https://doi.org/10.1080/21691401.2018.1489267>



Published online: 22 Jul 2018.



Submit your article to this journal [↗](#)



Article views: 94



View Crossmark data [↗](#)



Citing articles: 1 View citing articles [↗](#)



Metal nanoparticles restrict the growth of protozoan parasites

Oluoyomi Stephen Adeyemi^a , Nthatisi Innocentia Molefe^b, Oluwakemi Josephine Awakan^a, Charles Obiora Nwonuma^a, Omokolade Oluwaseyi Alejollowo^a, Tomilola Olaolu^a, Rotdelmwwa Filibus Maimako^a, Keisuke Suganuma^b, Yongmei Han^b and Kentaro Kato^b

^aMedicinal Biochemistry, Nanomedicine and Toxicology Laboratory, Department of Biological Sciences, Landmark University, Omu-Aran, Nigeria; ^bNational Research Center for Protozoan Diseases, Obihiro University of Agriculture and Veterinary Medicine, Obihiro, Hokkaido, Japan

ABSTRACT

The *Trypanosoma* and *Toxoplasma* spp, are etiological agents of diseases capable of causing significant morbidity, mortality and economic burden, predominantly in developing countries. Currently, there are no effective vaccines for the diseases caused by these parasites; therefore, therapy relies heavily on antiprotozoal drugs. However, the treatment options for these parasitic diseases are limited, thus underscoring the need for new anti-protozoal agents. Here, we investigated the anti-parasite action of nanoparticles. We found that the nanoparticles have strong and selective *in vitro* activity against *T. b. brucei* but moderate *in vitro* activity against *T. congolense* and *T. evansi*. An estimation of the *in vitro* anti-*Trypanosoma* efficacy showed that the nanoparticles had ≥ 200 -fold selective activity against the parasite versus mammalian cells. Moreover, the nanoparticle alloys moderately suppressed the *in vitro* growth of *T. gondii* by $\geq 60\%$. In our *in vivo* study, the nanoparticles appeared to exhibit a trypanostatic effect, but did not totally suppress the rat parasite burden, thereby failing to appreciably extend the survival time of infected animals compared with the untreated control. In conclusion, this is the first study to demonstrate the selective *in vitro* anti-*Trypanosoma* action of nanoparticles and thus supports the potential of nanoparticles as alternative anti-parasitic agents.

ARTICLE HISTORY

Received 30 March 2018
Revised 1 June 2018
Accepted 4 June 2018

KEYWORDS

Chemotherapy; infectious diseases; nanomedicine; trypanosomosis

Introduction

Trypanosoma and *Toxoplasma* are protozoan parasites responsible for diseases that cause significant morbidity, mortality and economic burden, predominantly in developing countries [1–3]. For example, African trypanosomosis is a lethal infectious disease for both humans and livestock; an epidemic of this infection would have a major impact on the economic development of sub-Saharan Africa [4]. The causative agents are hemoflagellated protozoan parasites (i.e. *Trypanosoma* species), which elicit fatal diseases in African mammalian hosts. The human African trypanosomiasis (HAT, also called sleeping sickness) is caused by *Trypanosoma brucei rhodesiense* and *Trypanosoma brucei gambiense*, whereas bovine Trypanosomosis or *nagana* is caused by *Trypanosoma brucei brucei* [5–7]. *Trypanosoma* infection is fatal if left untreated either in humans or animals. Chemotherapy is a major means of controlling the infection; however, the available treatment options have various shortcomings including limited efficacy, toxicity and the emergence of resistant strains of trypanosomes [2,8]. Melarsoprol, one of the few drugs effective against the second stage of the disease, is reported to cause encephalopathy in 10–15% of patients, and approximately 40% of these cases are fatal [9,10]. These highlight the need for innovative strategies to

combat trypanosomosis, which puts the health of more than 60 million people in the sub-Saharan Africa at risk annually [11]. Consequently, the lack of effective anti-*Trypanosoma* therapies, coupled with unsuccessful attempts at vaccine development due to antigenic variation, has stimulated the search for new chemotherapy for trypanosomosis. Therefore, new candidate drugs against trypanosomosis are urgently needed.

Toxoplasmosis is another parasitic disease that constitutes a huge public health challenge. Toxoplasmosis, which is caused by the intracellular parasite *Toxoplasma gondii*, is a common parasitic disease capable of infecting a range of hosts, including nearly one-third of the human population [12]. Current treatment options for toxoplasmosis patients are limited; they include the use of anti-malarial drugs or antibiotics, which often cause significant side effects [13]. Thus, as with Trypanosomosis, this infection represents large global burden that is further enhanced by the shortcomings of available therapeutic options. These factors underscore the need for better anti-*T. gondii* treatment and/or new treatment approaches. Taken together, new antiprotozoals are urgently required, as most of the current treatment options have limitations such as poor efficacy, drug resistance, toxicity, high cost or unsuitable pharmacokinetic properties [1].

The use of nanomaterials or nanoparticles for biomedical purposes is on the rise particularly because of their nanoscale size, which affords unique and remarkable properties that can be explored for various biomedical purposes [14]. For example, nanoparticles such as silver (AgNP), gold (AuNP) and platinum (PtNP) have good solubility and have been shown to have anti-microbial [15,16] and anti-parasitic activities [3,17–19]. Separate studies have demonstrated that these nanoparticles also have other bioactivities such as selective binding and enzyme inhibition [20–22]. We recently reported the potential of AuNP and AgNP to selectively inhibit recombinant target enzymes from *T. b. brucei* [23,24]. In addition, we reported the potential of inorganic nanoparticles to restrict the growth of *T. gondii* [3,25]. Taken together, these findings support the further biological profiling of nanoparticles in experimental parasitic infection. It is against this backdrop that the present study investigated the anti-*Trypanosoma* potential of several metal nanoparticles *in vitro* and *in vivo*. Alloys of these nanoparticles were also screened for anti-*T. gondii* activity *in vitro*.

Materials and methods

Nanoparticle synthesis and characterization

The nanoparticles were prepared as previously reported; AuNP, AgNP and PtNP were synthesized from HAuCl₄, AgNO₃ and H₂PtCl₆, respectively, and stabilized with tannic acid/ethanol [23,24,26,27]. Alloys of the nanoparticles (Ag-Au-Pt-NP, Ag-Pt-NP, Au-Pt-NP and Ag-Au-NP) were synthesized as previously reported [27] with little modification. Briefly, the individual salts (HAuCl₄, AgNO₃ or H₂PtCl₆) were reduced one after the other in ethanol using microwave-assisted heating to produce Ag-Au-Pt-NP, Ag-Pt-NP, Au-Pt-NP or Ag-Au-NP. The tryptophan-nanoparticle conjugates (AuNP^{TRP} and AgNP^{TRP}) were prepared as previously described and characterized [28]. The resulting coloured solutions (AgNP, pale yellow; AuNP, ruby red; PtNP, dark brown; Ag-Au-Pt-NP, dark-brown; Ag-Pt-NP, dark brown; Au-Pt-NP, dark wine red; Ag-Au-NP, brownish wine red; AuNP^{TRP}, wine-red; and AgNP^{TRP}, pale yellow) were filtered through 0.22- μ m filters and characterized by use of UV/Vis spectrophotometry, inductively coupled plasma optical emission spectrometry (ICP-OES), energy dispersive X-ray spectroscopy (EDX) and transmission electron microscopy (TEM) [23,24,26,27,29].

In vitro experiments

Trypanosoma parasites

Parasite culture conditions were as previously reported [8]. Briefly, *Trypanosoma congolense* IL3000, a savannah-type strain isolated near the Kenya/Tanzania border in 1966, *Trypanosoma evansi* Tansui and *T. b. brucei* GUTat 3.1 were maintained in the bloodstream form (BSF) in HMI-9 medium [30] and propagated at 33 °C (*T. congolense*) and 37 °C (*T. evansi* and *T. b. brucei*) in the air. The culture medium included Iscove's modified Dulbecco's medium (Sigma-Aldrich Japan, Tokyo, Japan) supplemented with 20% foetal bovine serum (FBS; Gibco, Invitrogen, Waltham, MA), 60 mM

HEPES (Sigma-Aldrich, St Louis, MO), 1 mM pyruvic acid sodium salt (Sigma-Aldrich, St Louis, MO), 0.1 mM bathocouproine (Sigma-Aldrich, St Louis, MO), 1 mM hypoxanthine, 16 μ M thymidine (HT supplement: Thermo Fisher Scientific K.K., Yokohama, Japan), 10 μ g/L insulin, 5.5 μ g/L transferrin, 6.7 ng/L sodium selenite (ITS-X: Thermo Fisher Scientific, Pittsburgh, PA), 0.0001% 2- β -mercaptoethanol (Sigma-Aldrich) and 2 mM L-cysteine (Sigma-Aldrich, St Louis, MO). The cultures were maintained by replacing the entire supernatant with fresh medium every other day.

In vitro evaluation of the anti-trypanosoma activity of nanoparticles

The *in vitro* evaluation for anti-*Trypanosoma* activity was performed as previously described [8]. Briefly, *T. congolense*, *T. b. brucei* and *T. evansi* were seeded at 1×10^5 , 1×10^4 and 2×10^4 cells/mL, respectively, in a NuncTM 96-well optical bottom plate (Thermo Fisher Scientific, Pittsburgh, PA) and exposed to various concentrations of nanoparticles (0 to 10 μ g/mL). The plates were incubated at 33 °C (*T. congolense*) and 37 °C (*T. b. brucei* and *T. evansi*). After a 72 h-incubation, 25 μ L of CellTiter-GloTM Luminescent Cell Viability Assay reagent (Promega Japan, Tokyo, Japan) was added and the plates were shaken for 2 min using an MS3 basic plate shaker (IKA[®] Japan K.K., Osaka, Japan) to facilitate cell lysis and the release of intracellular ATP. After a 10 min-incubation at room temperature, the ATP concentration was measured using a GloMax[®]-Multi+ Detection System plate reader (Promega Japan). The experiments were carried out in triplicate.

Cytotoxicity of the nanoparticles in mammalian cells

The cell viability assays were as described elsewhere [3,28]. Briefly, Human foreskin fibroblast monolayers (HFF; ATCC[®], Manassas, VA) cultured in Dulbecco's Modified Eagle Medium (DMEM; Nissui, Tokyo, Japan) and supplemented with GlutaMAXTM-1 (Gibco, Invitrogen, Waltham, MA), 10% (v/v) FBS (Gibco, Invitrogen, Waltham, MA) and penicillin and streptomycin (10,000 U/ml; Leicestershire, UK) were allowed to grow to confluence at 37 °C in a 5% CO₂ atmosphere. At confluence, the cells were harvested and seeded in clear 96-well plates (Nunc; Fisher Scientific, Pittsburgh, PA), at a density of 1×10^5 cells per well. After a 72 h-incubation at 37 °C in a 5% CO₂ atmosphere, various concentrations of the nanoparticles (0 to 10 μ g/mL) were added. Culture medium lacking the test compounds was added to the control well and the medium only well was used for background correction. After a further 72 h-incubation at 37 °C in a 5% CO₂ atmosphere, cell viability was determined by use of the CellTiter-Aqueous One Solution proliferation assay kit (Promega, Madison, WI) following the manufacturer's instructions. Briefly, the plates and their contents were equilibrated to room temperature. Then, 20 μ L of the CellTiter-Aqueous One reagent was added to each well. The contents were briefly mixed on an orbital shaker and then incubated at 37 °C in a 5% CO₂ atmosphere for 1–4 h. The absorbance signal was recorded at 490 nm by using a microplate reader

(MTP 500; Corona Electric, Hitachinaka Japan). The assay was repeated three times, in triplicate.

Toxoplasma gondii parasite strain

A luciferase-expressing parasite strain, *T. gondii* RH-2F (ATCC® 50839), was used for this study. The parasite was maintained by repeated passages in monolayers of HFF cells (ATCC®, Manassas, VA) cultured in DMEM (Nissui, Tokyo, Japan) and supplemented with GlutaMAX™-I (Gibco, Invitrogen, Waltham, MA), 10% (v/v) FBS (Gibco, Invitrogen, Waltham, MA) and penicillin and streptomycin (10,000 U/ml; Leicestershire, UK). The number of *T. gondii* tachyzoites was determined by using a luminescence-based assay of β-galactosidase (β-gal) activity expressed by the parasite strain RH-2F. To obtain a purified parasite suspension for the assays, infected cells were syringe-released using a 27-gauge needle in order to lyse them. The lysates were passed through a 5-μm filter to obtain parasite suspension free of host cell debris. The parasite suspension was then washed with fresh culture medium and parasite density was measured with a haemocytometer and adjusted for *in vitro* experimental infection analysis.

Anti-T. gondii potential of nanoparticles in vitro

The nanoparticles were screened for *in vitro* anti-*T. gondii* as previously described [3,28,31]. Briefly, purified parasite suspension plus various concentrations of the nanoparticles (0 to 10 μg/mL; reconstituted in culture medium prior to use) were added to growing HFF monolayers in 96-well solid white plates (Nunc; Fisher Scientific, Pittsburgh, PA). Untreated but infected cells served as controls, whereas the culture medium only well was used for background correction. Sulfadiazine (Sigma, St Louis, MO) and/or pyrimethamine (Wako Pure Chemical, Osaka, Japan) were included as positive drug controls. After the 48-h incubation at 37 °C in a 5% CO₂ atmosphere, the viability of the RH-2F parasite strain was determined by assaying for β-gal activity by using a Beta-Glo luminescent assay kit (Promega, Madison, WI). The assay was performed in triplicate and repeated three times independently.

In vivo experiments

Parasite strain

T. b. brucei (Lafia strain) adapted to animal experimental trypanosomosis was used for this study. The Lafia strain of *T. b. brucei* was originally obtained from the Department of Veterinary and Livestock Studies, Nigerian Institute for Trypanosomiasis Research (NITR), Vom, Nigeria. The parasite was maintained by repeated passages in rats by inoculating 0.5 ml of parasite suspension (approximately 10⁶ trypanosomes/ml) into the peritoneal cavity of uninfected rats. The suspension usually contained 1 trypanosome per view at 10 × 40 magnification. Animals were inoculated with the parasite and parasitaemia was monitored daily to establish infection progress until the infected animals died.

Experimental animals

Male Wistar rats (weighting 150–160 g) were used as an experimental model of trypanosomosis. Caution was taken to ensure that all rats were germ- and disease-free. The animals were sourced from the small animal unit of the Department of Biochemistry, University of Ilorin, Nigeria. Animals were acclimatized for two weeks before commencement of the study.

Ethics statement

The animals were treated in accordance with approved guidelines for the handling of experimental animals and consistent with the International Guiding Principles for Biomedical Research Involving Animals. Geneva, Switzerland: (CIOMS) [32], under the observation of the local Institutional Ethics Committee on Scientific Research with approval and protocol 3152015.

Preliminary experiments

To establish the progress of infection in the animals, the rats were randomly divided into two groups as follows:

Group A: Uninfected and control

Group B: Infected with *T. b. brucei* and untreated

Parasite load was monitored daily to establish the progress of infection, until day 6 post-infection when infected animals died. To count the parasites, blood smears were made by collecting fresh blood from the tail vein of the animals and counting the parasites under a light microscopy (10 × 40 magnification) using the matching method of Herbert and Lumsden [33] as described elsewhere [34].

Anti-Trypanosoma evaluation of nanoparticles in vivo

After establishing the trend of events during infection by *T. b. brucei*, Wistar rats were assigned randomly into different groups with at least six animals per group. All animals were monitored daily for either parasite load or other physical changes. Treatment was assessed by determining the degree of reduction in parasite burden since parasite load correlates with severity of infection. DMZ and nanoparticle treatment commenced 96 h post-infection. Parasite load was monitored daily as previously reported [34]. The groupings were as follows:

Group 1: Uninfected and untreated

Group 2: Negative drug control (infected and untreated)

Group 3: Infected and treated with diminazene aceturate (DMZ; 3.5 mg/kg bw)

Group 4: Infected and treated with either gold, silver or platinum nanoparticles (5 μg/kg bw)

Group 5: Infected and treated with either gold, silver or platinum nanoparticles (10 μg/kg bw)

Data analysis

Data were analysed by using a one-way ANOVA (GraphPad Software Inc., San Diego, CA) and are presented as the mean \pm SEM. Comparisons among groups were determined by using a one-way ANOVA and Dunnett's post hoc test. p Values $\leq .05$ were considered to be statistically significant (GraphPad; CA). The concentration of the nanoparticles showing a 50% reduction in parasite and/or mammalian cell viability (i.e. EC_{50} and/or IC_{50} values) were estimated by using Prism 5 (GraphPad; CA); non-linear regression analysis was used to fit the curve. The % parasite load in the animals was plotted as a function of the days/concentrations of nanoparticle or drug used.

Results

The UV/Vis spectra and TEM images of the nanoparticles (Figures 1 and 2) conform with earlier reports [23,26,27] and thus confirm the successful synthesis of the nanoparticles. The TEM images revealed the nanoparticles as spherical in shape, while further analysis using ImageJ (National Institutes of Health, Bethesda, MD) revealed that the particles were polydispersed with diameter size ranges of 5–50 nm.

To establish the anti-parasite activity and mammalian cell cytotoxic potential of the nanoparticles (NPs), we screened the inorganic NPs at various concentrations between 0 and 10 $\mu\text{g}/\text{mL}$ for anti-*Trypanosoma* activity by incubating fresh parasite suspension (*T. b. brucei*, *T. congolense* and *T. evansi*) with the NPs for 72 h under the indicated cell culture conditions. Parasite growth curves were determined by measuring the ATP concentrations of the viable parasites by using a luminescence-based assay. To validate our assay for anti-*Trypanosoma* screening, we included pentamidine as a reference drug. This drug significantly inhibited the growth of *Trypanosoma* thus validating our assay. The NPs exhibited

differential anti-*Trypanosoma* potential among the three different species of *Trypanosoma*. For example, the gold and silver nanoparticles (AuNP and AgNP respectively) significantly reduced *T. b. brucei* viability by $\geq 95\%$ (Figure 3(A,B)), whereas AuNP was less effective against *T. congolense* and *T. evansi* with an average of $\leq 50\%$ parasite growth inhibition. AgNP reduced the growth of *T. congolense* and *T. evansi* by $\geq 70\%$, suggesting that these NPs may have different parasite targets. Further, the platinum nanoparticles (PtNP) was only effective against *T. congolense* (Figure 3(C)), with $\geq 50\%$ parasite growth inhibition. Although the NPs showed different anti-*Trypanosoma* action against the three species, there is no doubt that the anti-*Trypanosoma* activities of the NPs were strongly selective toward the parasite. An estimation of the ratio of the mammalian cell cytotoxic IC_{50} values to the anti-parasite EC_{50} values as a measure of the anti-parasite efficacy or selectivity index (SI) revealed a promising trend (Table 1); the NPs showed ≥ 200 -fold selectivity toward the various species versus the mammalian cell, indicating that the NPs may have specificity for *Trypanosoma* elimination. Furthermore, it should be noted that the EC_{50} values of these NPs are in the sub-microgram range.

Next, we asked whether combining the individual NPs as alloys would increase their anti-*Trypanosoma* efficacy. We screened NP alloys, including Ag-Au-Pt-NP, Ag-Pt-NP, Au-Pt-NP and Ag-Au-NP, for their potential to inhibit *Trypanosoma* growth. However, we found that the NP alloys failed to suppress parasite growth across the three species of *Trypanosoma*, exhibiting an average of $\leq 50\%$ parasite inhibition (Figure 4(A-D)). This finding may indicate that these NP alloys lack anti-*Trypanosoma* efficacy or that combining the individual NPs as alloys reduces their individual anti-parasitic action. Although, Ag-Au-NP moderately suppressed the growth of *T. b. brucei* by an average of $\geq 60\%$, there was no synergy among the NP activities when the NPs were combined as alloys. Moreover, some of the NP alloys showed

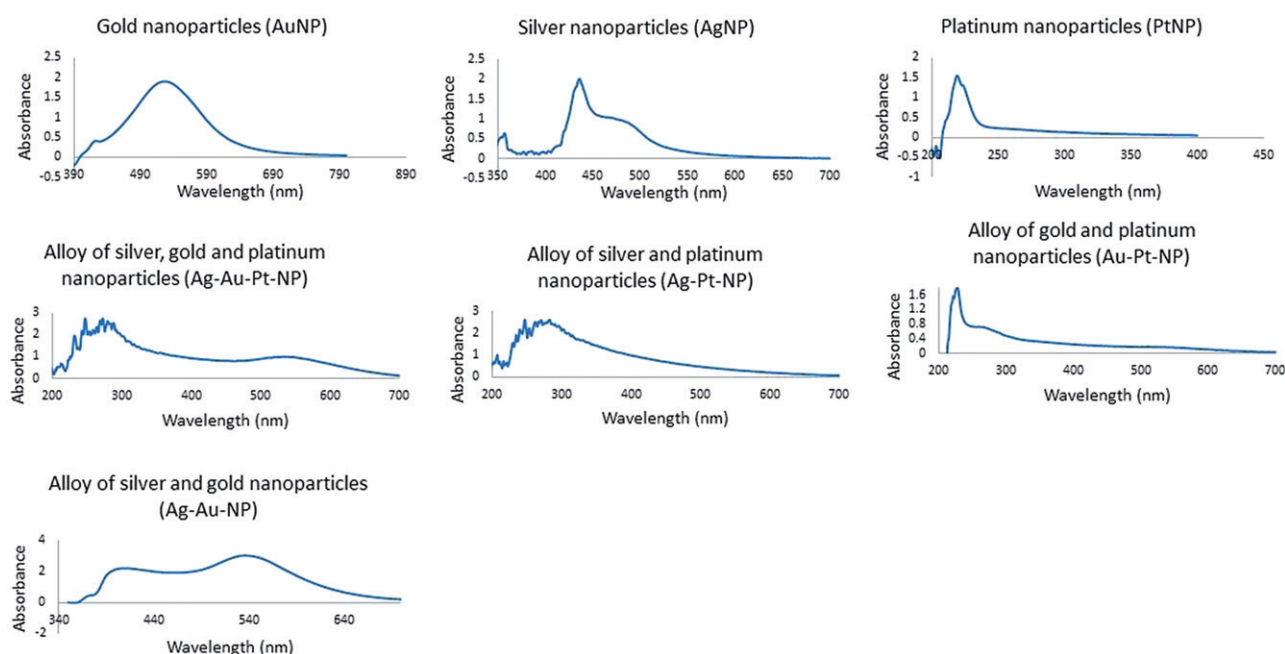


Figure 1. UV/Vis absorbance spectra of nanoparticles (200–800 nm).

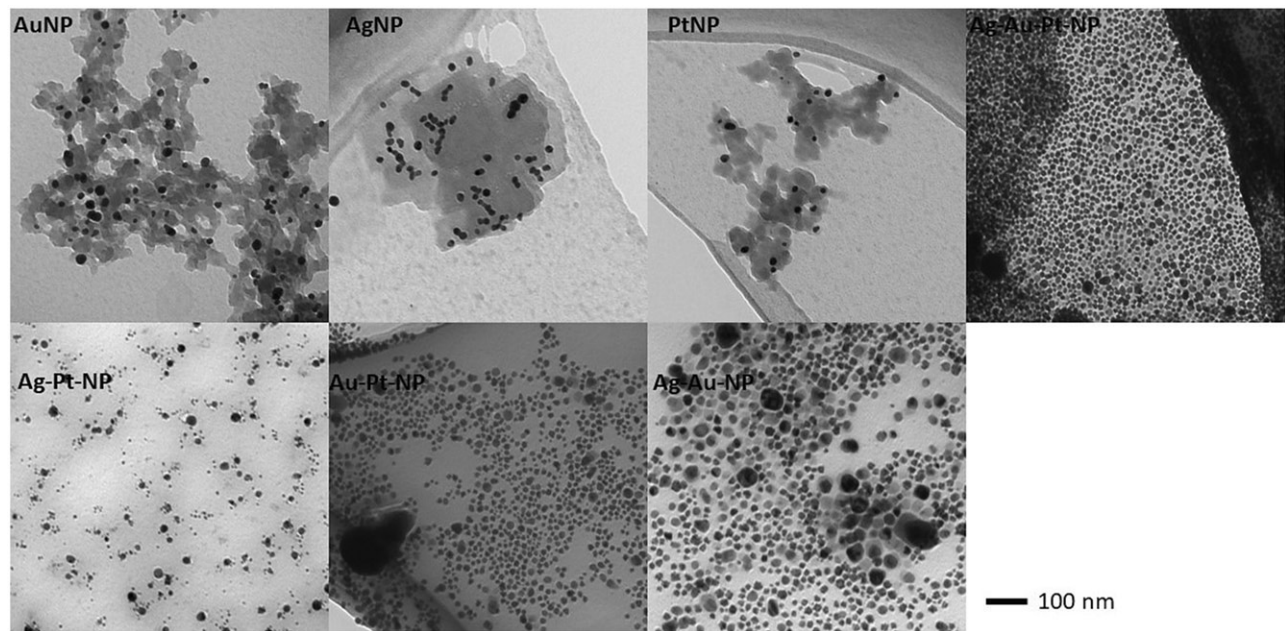


Figure 2. Transmission electron microscopy (TEM) images of nanoparticles. Scale bar =100 nm.

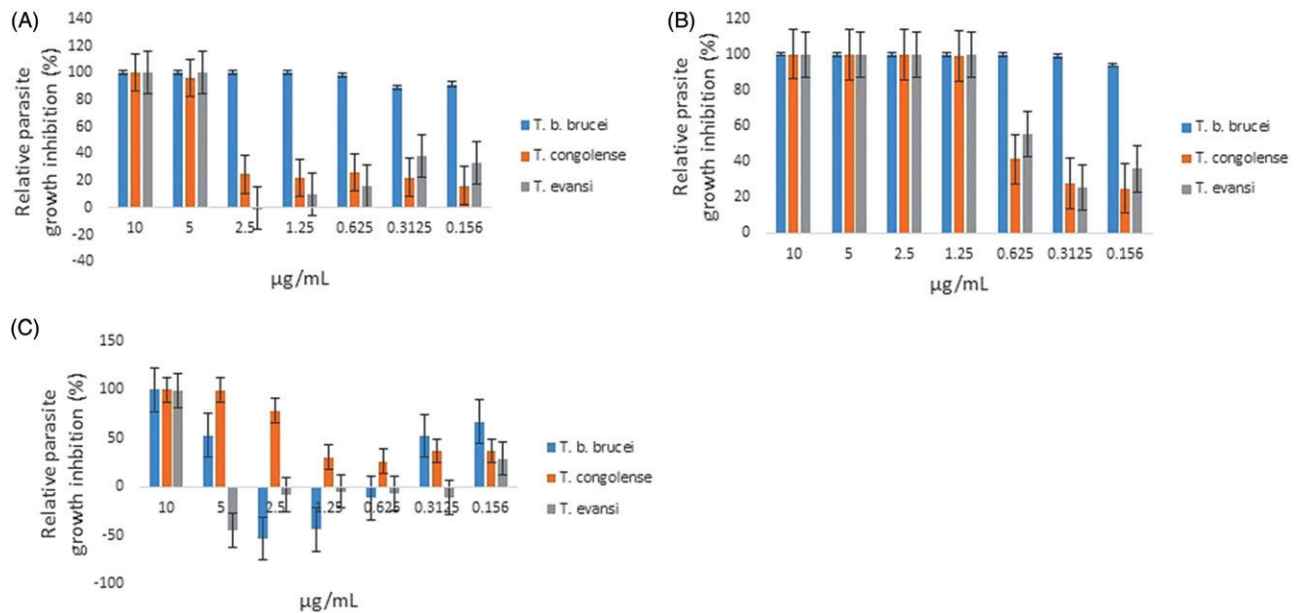


Figure 3. *In vitro* anti-*Trypanosoma* activity of nanoparticles: (A) AuNP; (B) AgNP; (C) PtNP. Values are expressed as the mean + standard error of the mean (SEM). Growth viability of parasites was determined after a 72-h incubation at 33 °C (*T. congolense*) or 37 °C (*T. b. brucei* and *T. evansi*) using Luminescent Cell Viability Assay reagent (Promega Japan, Tokyo, Japan). The experiment was repeated three times independently.

Table 1. Estimation of anti-parasitic efficacy of nanoparticles (µg/ml).

Compounds	EC ₅₀ <i>T. b. brucei</i>	EC ₅₀ <i>T. congolense</i>	EC ₅₀ <i>T. evansi</i>	EC ₅₀ <i>T. gondii</i>	IC ₅₀ HFF Cells	SI <i>T. b. brucei</i>	SI <i>T. congolense</i>	SI <i>T. evansi</i>	SI <i>T. gondii</i>
AuNP	≤0.001	≤0.08	≤0.12	–	≥97.63	≥2000	≥1000	≥800	–
AgNP	≤0.001	≤0.06	≤0.08	–	≥32.71	≥2000	≥500	≥400	–
PtNP	≤0.20	≤79.58	≤0.02	–	≥9.27	≤45	≤10	≤2	–
Ag-Au-Pt-NP	≤0.22	≤0.06	≤0.17	≤0.15	≥0.22	≤2	≤10	≤6	≤2
Ag-Pt-NP	≤0.66	≤0.03	≤0.04	≤0.15	≥0.24	≤2	≤1	≥500	≤2
Au-Pt-NP	≤1.65	≤0.02	ND	≤5.75	≥1.18	≤1	≥50	ND	≤1
Ag-Au-NP	ND	≤0.05	≤0.61	≤0.16	≥0.15	ND	≤5	≤1	≤1
AuNP ^{TRP}	ND	≤0.07	≤0.65	–	≥6.80	ND	≥90	≤15	–
AgNP ^{TRP}	ND	≤0.05	≤0.31	–	≥0.31	ND	≤10	≤1	–

Values presented are means (n = 3). The experiment was repeated three times independently. AuNP: gold nanoparticle; AgNP: silver nanoparticle; PtNP: platinum nanoparticle; ^{TRP}: tryptophan. * ND: not determined, SI: selectivity index (SI = IC₅₀ in mammalian cell divided by the EC₅₀ in parasite.).

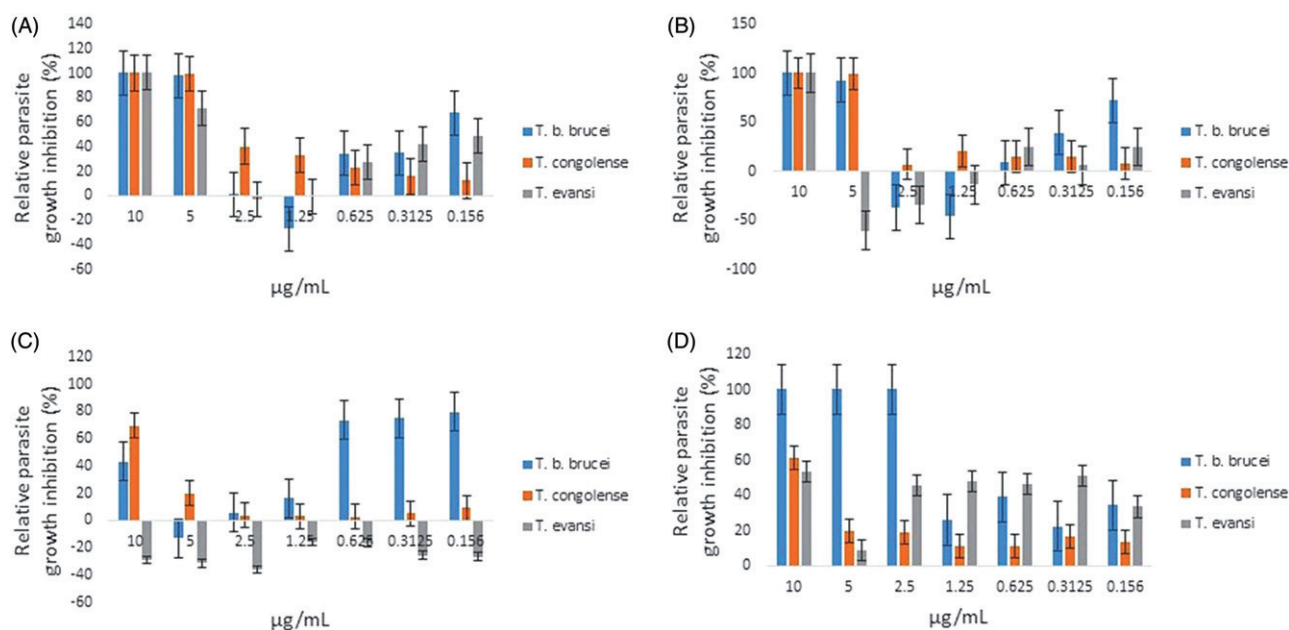


Figure 4. *In vitro* anti-*Trypanosoma* activity of nanoparticle alloy: (A) Ag-Au-Pt-NP; (B) Ag-Pt-NP; (C) Au-Pt-NP; (D) Ag-Au-NP. Values are expressed as the mean + standard error of the mean (SEM). Growth viability of parasites was determined after a 72-h incubation at 33 °C (*T. congolense*) or 37 °C (*T. b. brucei* and *T. evansi*) by using Luminescent Cell Viability Assay reagent (Promega Japan, Tokyo, Japan). The experiment was repeated three times independently.

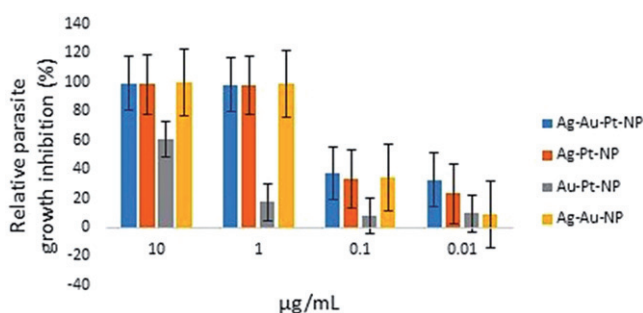


Figure 5. *In vitro* anti-*Toxoplasma gondii* activity of nanoparticle alloys. Values are expressed as the mean + standard error of the mean (SEM). Parasite growth inhibition was determined after a 48-h incubation at 37 °C/5% CO₂ by using a luciferase reporter assay. The experiment was repeated three times independently.

increased cytotoxicity toward the mammalian cells (Table 1) compared with the individual NPs. We previously reported that AuNP, AgNP and PtNP have anti-*T. gondii* activity [3]; therefore, we sought to determine how the NP alloys would affect *T. gondii* growth. All of the NP alloys moderately suppressed the *in vitro* growth of *T. gondii* by $\geq 60\%$ except for Au-Pt-NP (Figure 5). This finding contrasts with the poor anti-*Trypanosoma* activity exhibited by the same NP alloys (Figure 4(A–D)). Although the NP alloys had good anti-*T. gondii* activity, their selectivity toward the parasite versus the host mammalian cell was poor (≤ 2 -fold anti-parasitic action). This is far less than the ≥ 20 -fold selectivity earlier reported for the anti-*T. gondii* action of the individual NPs (AuNP, AgNP and PtNP). Sulfadiazine was included as reference drug for toxoplasmosis and, as expected, it restricted the growth of *T. gondii*, thus validating our assay.

We also sought to determine the anti-*Trypanosoma* activity of AuNP- and AgNP-tryptophan conjugates. This was premised on a recent report [28], that suggest that nanoparticle-tryptophan conjugates (AuNP^{TRP} and AgNP^{TRP}) had

better anti-*T. gondii* activity than nanoparticles lacking this amino acid. Therefore, we screened AuNP^{TRP} and AgNP^{TRP} for anti-*Trypanosoma* activity. Interestingly, both AuNP^{TRP} and AgNP^{TRP} appreciably suppressed the growth of *T. b. brucei* by $\geq 90\%$ (Figure 6(A,B)), but had no effect against *T. congolense* or *T. evansi* (≤ 20 and 40% parasite inhibition, respectively). This result is comparable to the anti-*Trypanosoma* activities of the NPs lacking l-tryptophan.

Lastly, we sought to evaluate the anti-*Trypanosoma* efficacy of the NPs *in vivo* by using a rat model of experimental infection. However, the results were not promising (Figure 7); there was no appreciable decline in the parasite burden for the NP-treated animals compared with the untreated control. Although it appeared that the NPs were trypanostatic, the NP treatments failed to clear the systemic parasite burden and consequently the animals succumbed to their infections in a manner comparable to the fate of the negative drug control group. However, diminazene aceturate treatment (3.5 mg/kg bw) not only reduced the systemic parasite burden but also significantly extended the survival time of the animals.

Discussion

The nanoscale size of nanoparticles confers unique and remarkable properties, such as enhanced solubility and large surface area-to-volume ratio, that can be explored for biomedical purposes [14]. Inorganic nanoparticles, such as silver and gold, have been shown to possess interesting properties such as anti-microbial activity [15,16,35], as well as the ability to modulate enzyme activities [20–22]. Previously, we reported the potential of AuNP and AgNP to selectively inhibit recombinant target enzymes from *T. b. brucei* [23,24]. On the basis of this finding as a view toward seeking better therapy for the treatment of trypanosomosis, we herein investigated the anti-parasite potential of these nanoparticles

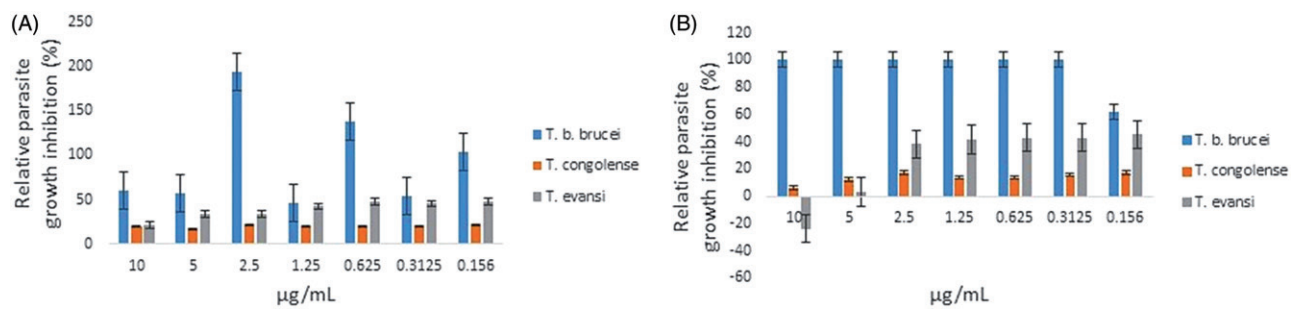


Figure 6. *In vitro* anti-*Trypanosoma* activity of nanoparticle-tryptophan conjugates: (A) AuNP^{TRP}; (B) AgNP^{TRP}. Values are expressed as the mean + standard error of the mean (SEM). Growth viability of parasites was determined after a 72-h incubation at 33 °C (*T. congolense*) or 37 °C (*T. b. brucei* and *T. evansi*) using Luminescent Cell Viability Assay reagent (Promega Japan, Tokyo, Japan). The experiment was repeated three times independently.

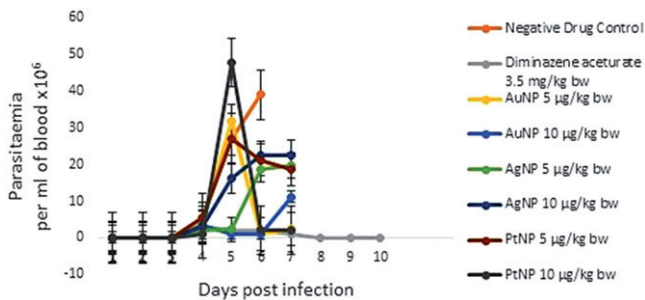


Figure 7. Anti-*Trypanosoma* effect of nanoparticles in rats. Values are expressed as the mean + standard error of the mean (SEM, $n = 5$). Treatment commenced at 96 h post-infection. Parasite burden was determined by counting the number of parasites in blood smears (made by collecting fresh blood from the tail vein of the animals) under a light microscope (100 \times magnification).

in vitro and *in vivo*. As a proof-of-principle, in the present study, we evaluated several nanoparticles (NPs) for their anti-parasitic potential against different *Trypanosoma* species and *Toxoplasma gondii*.

The NPs exhibited differential anti-*Trypanosoma* potential among the three different species of *Trypanosoma* tested. While AuNP was less effective against *T. congolense* and *T. evansi* with an average of $\leq 50\%$ parasite growth inhibition, AgNP reduced the growth of *T. congolense* and *T. evansi* by $\geq 70\%$, suggesting that these NPs may have different parasite targets. The finding that AuNP and AgNP showed better efficacy against *T. b. brucei* may support exploring these NPs as prospective treatment of the human type of trypanosomiasis caused by *T. b. rhodiense* and *T. b. gambiense*, given that *T. b. brucei* belongs to the same group and is closer in terms of morphological features to the human *Trypanosoma* pathogens. Taken together, AuNP and AgNP showed strong anti-*Trypanosoma* activity, consistent with previously published investigations of the anti-microbial and/or anti-parasite properties of AuNP and AgNP [3,16–19]. Similar studies using PtNP are scarce in the literature except for our recent report [3] that demonstrated the anti-*T. gondii* property of PtNP. Moreover, our findings herein support our earlier reports that AuNP and AgNP strongly and selectively inhibit recombinant *T. b. brucei* arginine kinase [23,24]. Arginine kinase is a phosphotransferase that is essential for the growth and survival of *T. b. brucei* particularly in the bloodstream of the infected host because it helps the parasite meet required energy demands to maintain a reductive environment [23]. Whether the NPs interact with this arginine kinase as a target in

suppressing the *in vitro* growth of *Trypanosoma* is yet to be determined, but the previous finding [23] indicated that arginine kinase might be a likely parasite target thus this warrants further investigation. Further, because the field of nanomedicine is still emerging, the modes of action of the majority of NPs are yet to be clearly defined. Nevertheless, studies have shown that the generation of reactive oxygen species (ROS) contributes considerably to the anti-parasitic action of NPs including AuNP, AgNP and others [3,36]. However, we cannot yet tell whether ROS production played a part in the action of the NPs against *Trypanosoma* in the present study. The differential efficacy of the NPs against the different species studied here may be connected to their mode of action, which would suggest that the NPs may affect different parasite targets across the three species of *Trypanosoma* investigated in this study. Furthermore, the NPs showed ≥ 200 -fold selectivity toward the various species versus the mammalian cell, suggesting that the NPs actually have specificity for *Trypanosoma* elimination.

In contrast, alloys of these nanoparticles failed to suppress parasite growth across all three species of *Trypanosoma* tested, exhibiting an average of $\leq 50\%$ parasite inhibition. The reason for this is unknown, but it does suggest that there is no synergy among the individual activities of the NPs when combined together as NP alloys. Conversely, the NP alloys moderately suppressed the *in vitro* growth of *T. gondii* by $\geq 60\%$, except Au-Pt-NP. Taken together, these findings indicate that AuNP, AgNP and PtNP are more effective individually than as alloys. Further, the findings suggest that AuNP and AgNP have potential as candidates for the treatment of *Trypanosoma*-related infection. This is the first study reporting the anti-*Trypanosoma* activities of these inorganic NPs and their alloys. Our findings herein support the anti-parasitic action of these NPs and are consistent with previously reported findings [3,16–19,37–40]. As further confirmation that inorganic NPs show promise as novel agents for the treatment of *T. b. brucei*-related infection, AuNP- and AgNP-tryptophan conjugates appreciably suppressed the growth of *T. b. brucei* by $\geq 90\%$ but had less activity against *T. congolense* and *T. evansi* (≤ 20 and 40% parasite inhibition, respectively). Whether this activity against *T. b. brucei* is attributable to the presence of l-tryptophan remains to be determined. However, recent findings from our laboratory revealed that AuNP- and AgNP-tryptophan conjugates have superior activity against *T. gondii* compared with ordinary

nanoparticles lacking the tryptophan [28]. It is likely that since *T. gondii* is auxotrophic for L-tryptophan and must therefore obtain it from the host in order to survive, the parasite becomes more sensitive to AuNP^{TRP} and AgNP^{TRP} leading to better anti-*T. gondii* activity compared with NPs that lack L-tryptophan. Whether the same mechanism is applicable in the present study is unclear. Although L-tryptophan is essential for the growth of trypanosomes, *T. gondii* is an intracellular parasite whereas *Trypanosoma* is extracellular.

The NPs did not effectively reduce the rat systemic parasite burden and consequently failed to extend the survival time of the infected rats. Probably, the NP doses (≤ 0.02 mg/kg bw) used in the present study were too low to be effective in this rat model of experimental trypanosomiasis. Our future investigations would seek to determine the *in vivo* anti-parasitic efficacy of these NPs by using higher doses than those used in the current study. Several studies have established that when orally administered, the LD₅₀ for AuNP, AgNP, as well as PtNP, is ≥ 500 mg/kg [26,41,42].

In conclusion, this is the first study to report the anti-*Trypanosoma* activity of inorganic NPs and their alloys. These findings add support to the *in vitro* anti-parasitic action of NPs against *T. b. brucei*, *T. congolense* and *T. evansi*. Our data also indicate that NPs may be effective against both extracellular and intracellular parasites. Although the present data do not support the *in vivo* efficacy of these NPs, future investigations to determine the *in vivo* anti-*Trypanosoma* effectiveness of these NPs at higher doses are warranted. Nevertheless, the NPs exhibited promising and selective *in vitro* anti-*Trypanosoma* action.

Disclosure statement

No potential conflict of interest was reported by the authors.

Funding

The authors acknowledge the International Foundation for Science (IFS) Grant F/5672 and the Japan Society for the Promotion of Science Fellowship.

ORCID

Oluyomi Stephen Adeyemi  <http://orcid.org/0000-0001-9342-8505>

References

- Creek DJ, Barret MP. Determination of antiprotozoal drug mechanisms by metabolomics approaches. *Parasitology*. 2014;141:83–92.
- Adeyemi OS, Sulaiman FA. Biochemical and morphological changes in *Trypanosoma brucei brucei*-infected rats treated with homidium chloride and diminazene aceturate. *J Basic Clin Physiol Pharmacol*. 2012;23:179–183.
- Adeyemi OS, Murata Y, Sugi T, et al. Inorganic nanoparticles caused death of *Toxoplasma gondii* through alteration of redox status and mitochondrial membrane potential. *Int J Nanomedicine*. 2017;12:1647–1661.
- Adeyemi OS, Akanji MA, Ekanem JT. Anti-anaemic properties of the ethanolic extracts of *Psidium guajava* in *Trypanosoma brucei* infected rats. *Res J Pharmacol*. 2010;4:74–77.
- Barrett MP, Boykin DW, Brun R, et al. Human African trypanosomiasis: pharmacological re-engagement with a neglected disease. *Br J Pharmacol*. 2007;152:1155–1171.
- Chappuis F, Udayraj N, Stietenroth K, et al. Eflornithine is safer than melarsoprol for the treatment of second-stage *Trypanosoma brucei gambiense* human African trypanosomiasis. *Clin Infect Dis*. 2005;41:748–751.
- Stijlemans B, Vankrunkelsven A, Brys L, et al. Role of iron homeostasis in trypanosomiasis-associated anemia. *Immunobiology*. 2008;213:823–835.
- Molefe NI, Yamasaki S, Macalanda AMC, et al. Oral administration of azithromycin ameliorates trypanosomiasis in *Trypanosoma congolense*-infected mice. *Parasitol Res*. 2017;116:2407–2415.
- Blum J, Nkunku S, Burri C. Clinical description of encephalopathic syndromes and risk factors for their occurrence and outcome during melarsoprol treatment of human African trypanosomiasis. *Trop Med Int Health*. 2001;6:390–400.
- World Health Organization. Control and surveillance of African trypanosomiasis: report of a WHO Expert Committee. *World Health Organ Tech Rep Ser*. 1998;881(I-VI):1–114.
- Gupta S, Igoillo-Esteve M, Michels PAM, et al. Glucose-6-phosphate dehydrogenase of trypanosomatids: characterization, target validation, and drug discovery. *Mol Biol Int*. 2011;2011:135701.
- Black MW, Boothroyd JC. Lytic cycle of *Toxoplasma gondii*. *Microbiol Mol Biol Rev*. 2000;64:607–623.
- Kamau ET, Srinivasan AR, Brown MJ, et al. A focused small-molecule screen identifies 14 compounds with distinct effects on *Toxoplasma gondii*. *Antimicrob Agents Chemother*. 2012;56:5581–5590.
- Adeyemi OS, Sulaiman FA. Evaluation of metal nanoparticles for drug delivery systems. *J Biomed Res*. 2015;29:145–149.
- MubarakAli D, Thajuddin N, Jeganathan K, et al. Plant extract mediated synthesis of silver and gold nanoparticles and its antibacterial activity against clinically isolated pathogens. *Colloids Surf B Biointerfaces*. 2011;85:360–365.
- Lekshmi NCJ, Sumi SB, Viveka S, et al. Antibacterial activity of nanoparticles from *Allium* sp. *J. Microbiol Biotech Res*. 2012;2:115–119.
- Bhardwaj R, Saudagar P, Dubey VK. Nanobiosciences: a contemporary approach in antiparasitic drugs. *Mol Cell Pharmacol*. 2012;4:97–103.
- Das S, Bhattacharya A, Debnath N, et al. Nanoparticle-induced morphological transition of *Bombyx mori* nucleopolyhedrovirus: a novel method to treat silkworm grasserie disease. *Appl Microbiol Biotechnol*. 2013;97:6019–6030.
- Rahul S, Chandrashekhar P, Hemant B, et al. *In vitro* antiparasitic activity of microbial pigments and their combination with phyto-synthesized metal nanoparticles. *Parasitol Int*. 2015;64:353–356.
- Wigginton NS, Titta A, Piccapietra F, et al. Binding of silver nanoparticles to bacterial proteins depends on surface modifications and inhibits enzymatic activity. *Environ Sci Technol*. 2010;44:2163–2168.
- Salma AA, Amer HA, Shaemaa HA, et al. The effects of gold and silver nanoparticles on transaminase enzymes activities. *Int J Cancer*. 2011;3:2249–2329.
- Srivastava M, Singh S, Self WT. Exposure to silver nanoparticles inhibits selenoprotein synthesis and the activity of thioredoxin reductase. *Environ Health Perspect*. 2012;120:56–61.
- Adeyemi OS, Whiteley CG. Interaction of nanoparticles with arginine kinase from *Trypanosoma brucei*: kinetic and mechanistic evaluation. *Int J Biol Macromol*. 2013;62:450–456.
- Adeyemi OS, Whiteley CG. Interaction of metal nanoparticles with recombinant arginine kinase from *Trypanosoma brucei*: thermodynamic and spectrofluorimetric evaluation. *Biochim Biophys Acta*. 2014;1840:701–706.
- Adeyemi OS, Murata Y, Sugi T, et al. Modulation of host HIF-1 α activity and the tryptophan pathway contributes to the anti-*Toxoplasma gondii* potential of nanoparticles. *Biochem Biophys Res*. 2017;11:84–92.

- [26] Adeyemi OS, Sulaiman FA, Akanji MA, et al. Biochemical and morphological changes in rats exposed to platinum nanoparticles. *Comp Clin Pathol*. 2016;25:855–864.
- [27] Pal A, Shah S, Devi S. Microwave-assisted synthesis of silver nanoparticles using ethanol as a reducing agent. *Mater Chem Phys*. 2009;114: 530–532.
- [28] Adeyemi OS, Murata Y, Sugi T, et al. Exploring amino acid-capped nanoparticles for selective anti-parasitic action and improved host biocompatibility. *J Biomed Nanotechnol*. 2018;14:847–867.
- [29] Sivaraman SK, Elango I, Kumar S, et al. A green protocol for room temperature synthesis of silver nanoparticles in seconds. *Curr Sci*. 2009;97:1055–1059.
- [30] Hirumi H, Hirumi K. *In vitro* cultivation of *Trypanosoma congolense* bloodstream forms in the absence of feeder cell layers. *Parasitology*. 1999;102:225–236.
- [31] Ishiwa A, Kobayashi K, Takemae H, et al. Effects of dextran sulfates on the acute infection and growth stages of *Toxoplasma gondii*. *Parasitol Res*. 2013;112:4169–4176.
- [32] Council for International Organizations of Medical Sciences. International guiding principles for biomedical research involving animals. Geneva, Switzerland: Council for International Organizations of Medical Sciences (CIOMS); 1985.
- [33] Herbert WJ, Lumsden WHR. *Trypanosoma brucei*: a rapid “matching” method for estimating the host's parasitemia. *Exp Parasitol*. 1976;40:427–431.
- [34] Adeyemi OS, Ekanem JT, Sulyman F. Depletion of parasitaemia by halofantrine hydrochloride and artemether in rats infected with African trypanosomes. *Afr J Pharm Pharmacol*. 2009;3:432–438.
- [35] Butkus MA, Labare MP, Starke JA, et al. Use of aqueous silver to enhance inactivation of coliphage MS-2 by UV disinfection. *Appl Environ Microbiol*. 2004; 70:2848–2853.
- [36] Saini P, Saha SK, Roy P, et al. Evidence of reactive oxygen species (ROS) mediated apoptosis in *Setaria cervi* induced by green silver nanoparticles from *Acacia auriculiformis* at a very low dose. *Exp Parasitol*. 2016;160:39–48.
- [37] Ahmad A, Syed F, Shah A, et al. Silver and gold nanoparticles from *Sargentodoxa cuneata*: synthesis, characterization and anti-leishmanial activity. *RSC Adv*. 2015;5:73793–73806.
- [38] Saad AHA, Soliman MI, Azzam AM. Antiparasitic activity of silver and copper oxide nanoparticles against *Entamoeba Histolytica* and *Cryptosporidium Parvum* cysts. *J Egypt Soc Parasitol*. 2015;45: 593–602.
- [39] Francis S, Joseph S, Koshy EP, et al. Microwave assisted green synthesis of silver nanoparticles using leaf extract of *elephantopus scaber* and its environmental and biological applications. *Artif Cells Nanomed Biotechnol*. 2018;46:795–804.
- [40] Vijayan R, Joseph S, Mathew B. *Indigofera tinctoria* leaf extract mediated green synthesis of silver and gold nanoparticles and assessment of their anticancer, antimicrobial, antioxidant and catalytic properties. *Artif Cells Nanomed Biotechnol*. 2018;46: 861–871.
- [41] Adeyemi OS, Faniyan T. Antioxidant status in rats orally administered silver nanoparticle. *J Taibah Uni Med Sci*. 2014;9:182–186.
- [42] Maneewattanapinyo P, Banlunara W, Thammacharoen C, et al. An evaluation of acute toxicity of colloidal silver nanoparticles. *J Vet Med Sci*. 2011;73:1417–1423.